Proceedings of the Fourth International Conference on Thermal Engineering: Theory and Applications January 12-14, 2009, Abu Dhabi, UAE

New Correlation Formulas to relate Heat Transfer in Wick Heat Pipe

Based on Experimental Study

Ali Kianifar, Farzad Samareh Mohammadian *

Department of Mechanical, Engineering Faculty, Ferdowsi University of Mashhad, Iran

Abstract

In this paper, an experimental investigation has been carried out to compare the thermal performances of a copper heat pipe with and without wick. Thermal performance of the heat pipe is affected by many factors such as: Inclination angle (from horizontal axis (φ)), Filling ratio (ratio of volume of working fluid to volume of evaporator section (FR)), Heat Input (Q) , Coolant flow rate $(\dot{m})$ and Permeability (K) are presented and discussed. The heat pipe was made from copper with methanol as the heat transfer fluid. Screen mesh 100ss(three layer) used for wick structure to return condensate to evaporator section. The comparison between results of a heat pipe with and without wick (thermosyphon) provided an important quantitative and qualitative understanding of the wick heat pipe performance. Empirical correlations for the heat transfer coefficients were obtained.

Keywords: Heat Pipe, Wick, Heat Transfer, Permeability, Filling Ratio.

1. Introduction

The heat pipe has been widely applied for cooling and heat spreading applications due to its superior heat conductivity. It utilizes the large latent heat associated with phase change and a large quantity of heat can be transferred from the evaporator section to the condenser section with a relatively small temperature difference.

Heat pipes can have a thermal conductance tens of times greater than the best metallic conductors.This is because the heat transfer in a heat pipe utilizes the phase change of the working fluid, where a high amount of heat can be transferred with very little temperature difference between source and sink.

The wick structure of the heat pipe generates a capillary pressure, which is dependent on the pore radius of the wick and the surface tension of the working fluid and provides capillary forces that the condensate back to the hot end of the heat pipe and thereby complete the continuous evaporation/condensation cycle.[1],[2]

2. Content

2.1.Theory for porous media

In the fluid mechanics of porous media, the place of momentum equation or force balances as the Darcy law can be written(in the presence of a body force):[3]

$$u = \frac{K}{\mu}\left(-\frac{dP}{dx} + \rho g_x\right) \qquad (1)$$

u Velocity, m/s

K Permeability, m^2

ρ Mass density , kg/m^3

μ Dynamic viscosity, $kg/m-s$

$\frac{dP}{dx}$ Pressure gradient

It is a well-known fact that in heat pipe pressure balance, loss of pressure through the wick is a significant factor. Wick permeability K is in direct correlation with wick structure porosity ε , is usually given by: [1]

$$K = \frac{2\varepsilon r_h^2}{f_l \,\mathrm{Re}_l} \qquad (2)$$

ε Wick porosity, $[V_P/V_t]$

r_h Hydraulic radius, m

Re_l Reynolds number based on hydraulic diameter, $[\varpi D_h / \nu]$

f_l Skin friction coefficient, $[2\tau_\omega / \rho\varpi^2]$

V_P Pore volume, m^3

V_t Total volume of the wick structure, m^3

Capillary wick structures have been placed inside thermosyphons for several reasons: to decrease the vapor-liquid interaction which causes flooding, to aid in the circumferential distribution of liquid in a tilted thermosyphon, to promote nucleate boiling sites in the evaporator and to enhance condensation heat transfer in the condenser section. [1]

The experimental facilities are described in the text section, followed by a discussion of the results and the conclusions from this study.

2.2.Description of experiments procedures

For experimental investigation of heat transfer specifications the copper heat pipe has been fabricated and a gauge was positioned at the end cap to put the wick inside the pipe easily.

* Corresponding author: +985117615134,+989153222832
E-mail: farzad_samareh@yahoo.com

In this experiment a copper tubes of 1000 mm long with inside diameter of 16 mm and 2 mm thickness were employed. The working length of the heat pipe consists of three parts; the lower part 430 mm as the evaporator section, the middle part 160 mm as the adiabatic section, and the upper part 410 mm as the condenser section. The 410 mm long, water jacket surrounding the condenser section. Inlet and outlet connections located obliquely across each other to introduce swirl flow. Eight Ni-Cr thermocouples were installed mechanically to the surface of the evaporator and adiabatic and condenser to monitor the temperature distribution. A personal computer and a data logger were used to show the temperatures measured by thermocouples. The heat pipe was surrounded by 40 mm thickness of glass wool for insulating and stopping the heat transfer to the environment. The source of the heat is a 1000W electric heater, wrapped around the lower end of the heat pipe (evaporator) and the accuracy of monitoring for voltage and ampere was $\pm 2\%$. The heater power of evaporator was calculated by multiplying the voltage and the current measured from the digital multi-meter. The temperature of inlet and outlet coolant water measured by digital thermometer and also the mass flow rate of water was measured by a rotameter. The presence of non-condensable-gases (NCG) in a heat pipe can cause a general failure of the capillary. In this system, a vacuum pump is connected to the heat pipe and discharged the NCG as much as possible. Table.1 shows the specifications of the heat pipe for this study.

Table1.Geometrical and physical parameters of Heat Pipe

Inner/outer diameter	16/20mm
Evaporator length	430mm
Condenser length	410mm
Adibatic length	160mm
Porous wick	*Screen mesh 100ss*
Mean pore radius	*0.0131 cm*
Permeability	$1/523\times10^{-10}\mathrm{m}^2$
Porosity	50%
Working fluid	*Methanol*
Heat Input	100,150,200w
Inclination angle	30,50,70,90
FR(%)	35,65,80,95

During this experiment thermocouples signals are continuously detected in form of chart on monitor. At this point in the tests, it took approximately 30 min to reach steady state. Once the steady-state condition has been reached, the temperature distribution along the heat pipe is measured and recorded, along with the other experimental parameters. The accuracy of temperature measurement was at range of $\pm 1^{\circ C}$.

The measured parameters were: heat input of the evaporator section(Q_{in}), heat output of the condenser section(Q_{out}), temperature of inlet and outlet of coolant water, the mass flow rate of coolant water, and surface temperatures of evaporator, adiabatic and condenser sections. The experimental limits were as follows:

- Heat input (Q_{in}) between 100 and 200 W
- Filling ratio (FR) between 35 and 100%
- Inclination angle (φ) between 30° and 90°
- Flow mass rate ($\dot{m}$) between 0.00997 and 0.0299 kg/s

The schematic of the test rig used in this work is shown in Fig.1

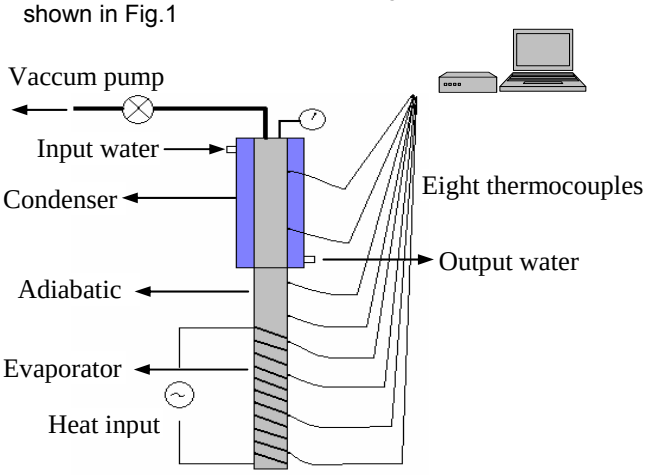

Fig. 1. A schematic diagram of the tested heat pipe

2.3. Heat transfer coefficient inside the Heat Pipe

The heat transfer in the condenser section was found to be only by conduction. In the evaporator, however, either conduction or boiling heat transfer can occur. A number of investigations have shown that the heat transfer in the condenser section does appear to be conduction, and most models assume the same is true in the evaporator.[1,2,4]

The rate of heat transfer to the evaporator section of a Heat Pipe can be calculated from the Eq. (3)

$$Q_{in} = VI \quad (3)$$

Q_{in} Input heat into the evaporator section, W

V Voltage, V

I Current, A

Heat transfer coefficient obtained from Eq.(4)

$$Q_{in} = h_e A_e (T_{e,m} - T_v) \quad (4)$$

h_e Heat transfer coefficient of evaporator, W/m^2K

A_e Evaporator heated surface, m^2

$T_{e,m}$ Average of steady temperature in evaporator, $^\circ C$

T_v Average of steady temperature in adiabatic, $^\circ C$

The experimental heat transfer coefficient of laminar film in condenser of a heat pipe is:

$$h_c = \frac{Q_{out}}{A_c (T_v - T_c)} \quad (5)$$

Q_{out} Transmitted heat from the condenser, W

h_c Heat transfer coefficient of condenser, W/m^2K

T_c Average of steady temperature in condenser, $^\circ C$

A_c Condenser surface, m^2

Rohsenow reported a model for nucleate boiling as:[5]

$$q_s = \mu_l A h_{fg} \left[\frac{g(\rho_l - \rho_v)}{\sigma} \right]^{1/2} \left(\frac{c_{pl}(T_e - T_v)}{C_{sf} h_{fg} \,\mathrm{Pr}^n} \right)^3 \quad (6)$$

And $q_s = h_e (T_e - T_v)$ (7)

C_{sf} The solid-fluid constant,[0.0068 for water-copper]

n [1 for water-copper]

Pr Prandtl Number,$[\nu/\alpha]$

The correlation that Imura suggests for the evaporator section of a two phase closed thermosyphon is: [6]

$$\bar{h}_e = 0.32\left(\frac{\rho_l^{0.65} k_l^{0.3} c_{pl}^{0.7} g^{0.2} q_e^{0.4}}{\rho_v^{0.25} h_{fg}^{0.4} \mu_l^{0.1}}\right)\left(\frac{p_v}{p_{atm}}\right)^{0.3} \quad (8)$$

And Q_{out} in the condenser obtained from Eq.(9)

$$Q_{out} = \dot{m} c_p (T_{wo} - T_{wi}) \quad (9)$$

$\dot{m}$ Coolant water flow rate, kg/s

c_p Specific heat at constant pressure, $J/(kg-K)$

T_{wo} Outlet water temperature of condenser, $^\circ C$

T_{wi} Inlet water temperature of condenser, $^\circ C$

Fig.2 shows the experimental setup for the measurement of thermal performances of the heat pipe.

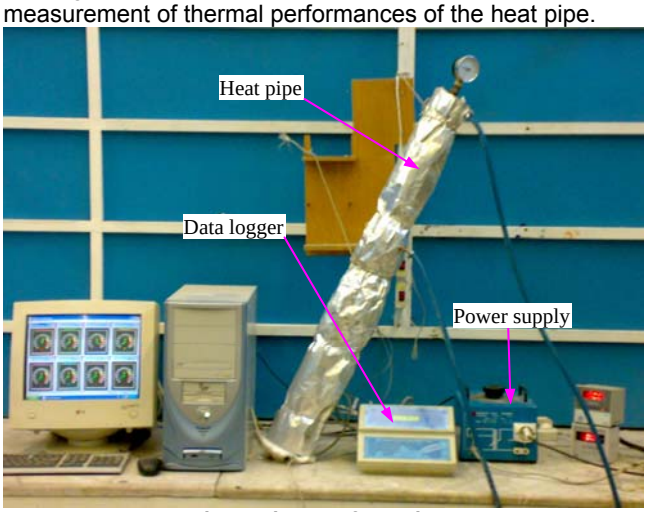

Fig. 2. Picture of test rig

2.4. Operating Limitation

Since the heat pipe benefits from the phase change of the working fluid, the thermodynamics of the process are critical. The operation of the heat pipe is limited by several operating phenomena. Each of these limitations is dependent on the wick structure, working fluid, temperature, orientation, and size of the heat pipe. Below is a brief description of each of the limitations:

2.4.1. Boiling Limit

As more heat is applied to the heat pipe at the evaporator, bubbles may be formed in the evaporator wick. The formation of vapor bubbles in the wick is undesirable because they can cause hot spots and obstruct the circulation of the liquid. As the heat flux is increased, more bubbles are formed. At a certain heat flux limit, the bubble formation completely blocks the liquid flow. This limitation is associated to a radial heat flux (heat is applied to the perimeter of the heat pipe). The boiling limitation is typically a high temperature phenomenon.

In order that a bubble can exist and grow in a superheated liquid, its size must be larger than a critical value. Following equation gives the relation for the critical size of a bubble or nucleus under a certain liquid superheat and physical properties:[1]

$$R_b \geq \frac{2\sigma T_{sat}}{h_{fg}\rho_{v,sat}\Delta T} \quad (10)$$

R_b Radius of vapor bubble, m

σ Surface tension, N/m

T_{sat} Saturation temperature of the evaporator, $^\circ C$

ΔT Temperature difference, $[T - T_{sat}]$

h_{fg} Latent heat of evaporation, J/kg

The analysis of the boiling limit involves the theory of bubble nucleation and growth. The analysis yields and expression for the heat transfer rate of the evaporator required to support a nucleate bubble as:[9]

$$Q_e = \frac{k_{eff} L_e w}{t} \frac{T_v}{h_{fg}\rho_v}\left(\frac{2\sigma}{R_b} - \Delta P_c\right) \quad (11)$$

Q_e Heat transfer rate, W

k_{eff} Effective thermal conductivity of wick, $W/(m-K)$

L_e Evaporator length, m

ΔP_c Capillary differential pressure, N/m^2

t Thickness of wick, m

Nucleation theory dictates that there is a minimum value for the initial radius of vapor bubble[10]. This is dependent upon fluid properties and surface conditions.

If the radius of vapor bubble is smaller than the radius required to sustain bubble growth, the vapor bubble will collapse.

2.4.2. Capillary Limit

The capillary pressure generated by the wick must be greater than the sum of the gravitational losses, liquid flow losses through the wick, and vapor flow losses. The liquid and vapor pressure drops are a function of the heat pipe and wick structure geometry (wick thickness, effective length, vapor space diameter, etc) and the fluid properties (latent heat, density, viscosity, etc). A critical heat flux exists that balances the capillary pressure with the pressure drop associated with the fluid and vapor circulation.

Chi proposes a pressure balance amongst the wick and vapor core within the heat pipe as expressed in Eq(12)[9]

$$\Delta P_c = \frac{2\sigma}{r_{eff}} = \Delta P_l + \Delta P_v + \Delta P_b \quad (12)$$

ΔP_c Capillary differential pressure, N/m^2

ΔP_l Pressure differential of liquid, N/m^2

ΔP_v Vapor differential pressure, N/m^2

ΔP_b Bulk force differential pressure, N/m^2

r_{eff} Effective pore radius, m

Substituting the Young-Laplace equation for ΔP_C, Darcy's law for ΔP_L, hydrostatic pressure due to gravity for ΔP_b, and the steady state closed system energy equation to relate mass flow rate and heat transfer rate and re-arranging yields an expression for the capillary heat transfer limit:[9]

$$Q_{cap,\max} = 2\left(\frac{KA}{r_{eff} L_{eff}}\right)\left(\frac{h_{fg}\sigma\rho\cos(\theta)}{\mu}\right)\left(1 - \frac{r_{eff}\rho g L \sin(\phi)}{2\sigma\cos(\theta)} - \Delta P_v\right) \quad (13)$$

ϕ Inclination angle from horizontal, degree

θ Wetting angle of liquid-solid-vapor, degree

L_{eff} Effective length of the wick, $[0.5L_e + L_a + 0.5L_c]$,m

A Cross-sectional area of wick, m^2

K Permeability, m^2

r_{eff} Effective radius of the porous wick, m

L Overall length of heat pipe, m

The pressure drop of the vapor can be expressed using the appropriate correlation such as Hagen-Poiseuille flow for the geometry of the vapor space within the heat pipe.

Eq. (13) represent the heat transfer rate as a function of wick properties, represented by the first bracketed term,

working fluid properties and its interaction with the wick solid's surface, represented by the second bracketed term, and the impact of bulk forces, represented by the third bracketed term.

For horizontal or against gravity (evaporator at a higher elevation than the condenser), the capillary limit is the heat pipe limit. For gravity aided orientations, the capillary limitations may be neglected, and the flooding limit may be used if the heat pipe can have an excess fluid charge. The maximum heat transport in moderate temperature applications is limited by the capillary pressure that can be generated by the wick structure.

Calculation formula for capillary limit :[1]

$$Q_{cap,\max} = \frac{2\sigma/r_{eff} - \rho_l g L \sin\phi}{F_l + F_v} \quad (14)$$

$$F_l = \frac{\mu_l}{\rho_l A_w K h_{fg}} \quad (15)$$

$$F_v = \frac{(f\,\mathrm{Re}_V)\mu_V}{2R_v^2 A_v \rho_V h_{fg}} \quad (16)$$

F_l Liquid frictional coefficient

F_v Vapor frictional coefficient

f Skin friction coefficient, $[2\tau_\omega/\rho\varpi^2]$

Re_V Local vapor Reynolds number, $[\varpi_v D/\nu_v]$

A_v Cross-sectional area of vapor flow passage, m^2

A_w Wick cross-sectional area, m^2

Since the vertical heat pipe is used, the pressure difference between liquid and vapor are very small with respect to the total capillary and gravity head.

2.4.3. Entrainment limit

Since the vapor and the liquid move in opposite directions in a heat pipe, a shear force exists at the liquid-vapor interface. If the vapor velocity is sufficiently high, a limit can be reached at which the liquid will be torn from the pores of the wick and entrained in the vapor. When enough fluid is entrained in the vapor that the condensate flow is stopped, abrupt dry-out of the wick at the evaporator results. The corresponding heat flux that results in this phenomenon is called the entrainment limit.

This limit obtained from following relation:[1]

$$Q_{entrainment,\max} = A_v h_{fg}\left(\frac{\sigma\rho_v}{2R_{h,w}}\right)^{1/2} \quad (17)$$

$R_{h,w}$ Hydraulic radius of the wick surface pore, $[\frac{2A_{lv}}{P}]$

[0.5W], W is the wire spacing for screen wicks

A_v Cross-sectional area of vapor flow passage, m^2

A_{lv} Area of individual surface pores of the wick, m^2

2.4.4. Sonic Limit

In a heat pipe of constant vapor space diameter, the vapor flow accelerates and decelerates because of the vapor addition in the evaporator and the vapor removal in the condenser. The changes in vapor flow also change the pressure along the heat pipe. As more heat is applied to the heat pipe, the vapor velocities generally increase. A choked flow condition will eventually arise, where the flow become sonic. At this point, the vapor velocities can not increase and a maximum heat transport limitation is achieved. The heat flux that results in choked flow is considered the sonic limit. The formula for the sonic limit, obtained by Levy has the following form:[8]

$$Q_{sonic,\max} = \frac{\rho_v c_v h_{fg} A_v}{\sqrt{2(K'+1)}} = A_v \rho_v h_{fg}\left[\frac{K' R_g T_v}{2(K'+1)}\right]^{1/2} \quad (18)$$

c_v Speed of sound, m/s

K' Ratio of specific heats, $[c_p/c_v]$

R_g Gas constant, $J/(kg-K)$

Busse obtained the following relation for the specific heat transfer at the sonic limit when the pipe operates in the regime produced by inertial effects:[7]

$$Q_{sonic,\max} = 0.474 h_{fg} A_v (\rho_v P_v)^{1/2} \quad (19)$$

A_v Cross-sectional area of vapor flow passage, m^2

ρ_v Vapor density, kg/m^3

P_v Vapor pressure, N/m^2

2.4.5. Viscous Limit

At low temperature viscous forces has shown that the axial heat flux increases as the pressure in the condenser is reduced, the maximum heat flux occurring when the pressure is reduced to zero. Busse derived the following question:[7]

$$Q_{viscous,\max} = \frac{R_v^2 h_{fg} \rho_v P_v}{16\mu_v L_e} \quad (20)$$

R_v Vapor space radius, m

L_e Effective heat pipe length, m

2.5. Results and discussion

2.5.1. Heat Transfer limits

Theoretical analysis of the heat transfer limitations were carried out by employing Eqs.(14),(17),(19)and (20). We found out that there is no limits of heat transfer inside the wick heat pipe and the thermosyphon.

2.5.2. Temperature distribution

The temperatures at four points on the evaporator section, two points on the adiabatic section, and two points on the condenser section, are simultaneously monitored to observe the temperature distribution over the entire length of the heat pipe with and without wick. The mean evaporator wall temperature reported here was estimated using all the data points, except one thermocouple that showed a lower temperature from the others in the evaporator. Excluding this data point in computing the mean, however, did not significantly change any results or the interpretation therein.

The temperature distribution of the wick heat pipe and thermosyphon are shown in Fig.3 in order to compare clearly. The wick heat pipe's temperature distribution is more uniform.

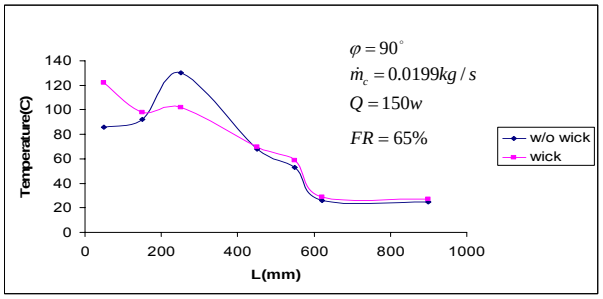

Fig. 3. Temperature distribution along the heat pipe with and without wick

Temperature distribution along the wall of the wick heat pipe and the thermosyphon in the evaporator section are almost isothermal. The measured temperature along the condenser showed lower values. This drop of temperature is expected because of the internal resistances due to boiling and condensation for both. However conductivity of the wick made the condenser temperature of the wick heat pipe a little bit higher than the thermosyphon.

2.5.3. Heat transfer coefficient of evaporator

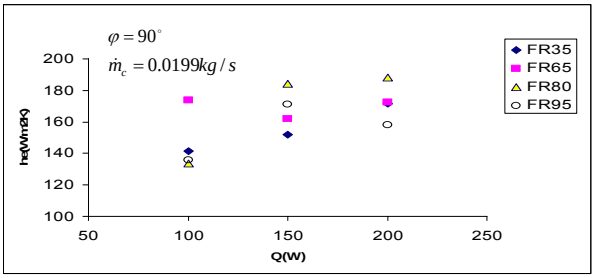

Fig. 4. Variation of heat transfer coefficient of evaporator with heat input for different filling ratio of the Wick heat pipe

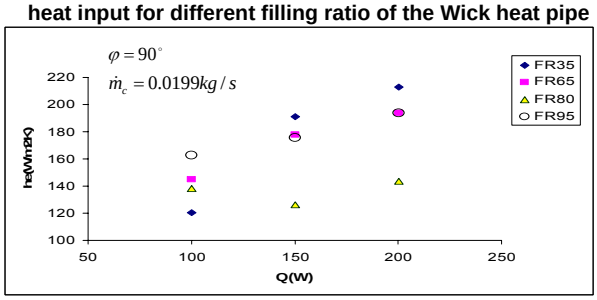

Fig. 5. Variation of heat transfer coefficient of evaporator with heat input for different filling ratio of the Thermosyphon

As shown in Figs.4,5 the heat transfer coefficient of evaporator increased as heat input increased. It is evident that for both, the wick heat pipe and the thermosyphon, heat transfer coefficient increase is proportional to the applied power. As mentioned earlier, due to existence the nucleate boiling, there was a considerable change in boiling regime when heat input increased.

The Figs.6,7 and 8 show that the effect of filling ratio manifested on the heat transfer coefficient. We observe, by increasing the filling ratio in the wick heat pipe, heat transfer coefficient of evaporator is slightly increased and nearly negligible. Theoretically, Wick extends nucleate boiling sites in the evaporator and it causes more working fluid vaporizes. Hence the temperature difference between evaporator and vapor decrease and lead to increase heat transfer coefficient.

In contrast to this, by decreasing the filling ratio, heat transfer coefficient of evaporator in the thermosyphon is increased. This effect is defined as, when filling ratio decreased, the contact between vapor and tube wall was considerably extended. Therefore the temperature difference between evaporating surface and vapor reduced and heat transfer coefficient achieved a higher value. As these effects are directly related to the charging of the working fluid, the filling ratio was the key factor affecting the operating temperature of wick heat pipe and thermosyphon, even so we should consider the minimum filling ratio to prevent any dry-out in the evaporator.

The sudden increase of the heat transfer coefficient at FR95% was shown in Figs.6,7 and 8 for the thermosyphon. The temperature difference between evaporator and adiabatic section could be influenced by the filling ratio. When filling ratio was too close to adiabatic section, at this point, it is difficult to calculate the exact temperature of adiabatic section. There is a high probability that small temperature difference due to this simple effect makes an unexpected rise in heat transfer coefficient.

Note that heat transfer coefficient in evaporator increased from FR35% to FR65% in Fig.6 in the thermosyphon. The effect of geyser boiling is significant in thermosyphon. Since the heat input is insufficient to cause steady nucleate boiling, the temperature of the liquid pool increases until it becomes superheated. At this point, a vapor bubble appears somewhere in the liquid pool, and its size quickly reaches the diameter of the pipe. As the bubble continue to grow in size, a slug of liquid on top of the bubble is propelled toward the condenser end cap. This sudden surge causes the vapor above the liquid slug to collapse, and the liquid slug may strike the condenser end cap with a smacking sound. Similar to a water hammer or steam hammer. After the slug of liquid strikes the condenser end cap, the liquid falls back to the evaporator section as a thin film, during which time it is sub-cooled. After a period of time, the liquid in the pool is again superheated, and the geyser boiling phenomenon continues. While this is usually a temporary condition during startup, it could cause a rupture of the container if it occurs frequently. Geyser boiling should be avoided because damage to the container wall may occur due to the slug of liquid striking the condenser end cap.[1]

The period of geyser boiling is shorter if the filling ratio is small and the severity of the slug striking the end cap is lessened. As the filling ratio increased, the period of geyser boiling increased. The contingency of geyser boiling is a crucial factor for temperature readings and stability of operation. When geyser boiling happened, sudden rise in evaporator temperature occurred. In consequence the temperature difference between evaporator and adiabatic increased and heat transfer coefficient of evaporator decreased in the thermosyphon.

In the wick heat pipe, the bubbles usually broke before they grow and reached the condenser end cap. Based on the present study, it is found that by using wick heat pipe, geyser boiling doesn't occur.

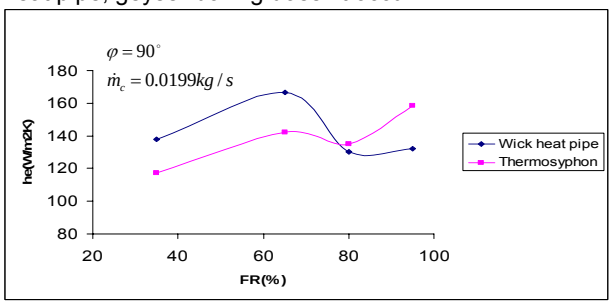

Fig. 6. Variation of heat transfer coefficient of evaporator with filling ratio for Q=100w

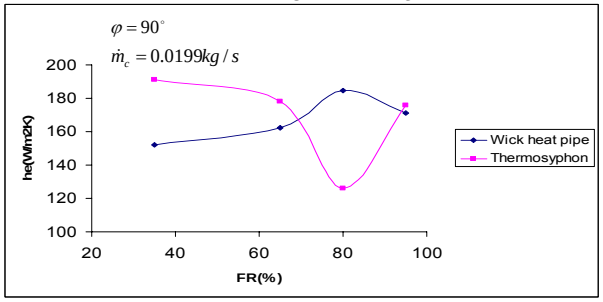

Fig. 7. Variation of heat transfer coefficient of evaporator with filling ratio for Q=150w

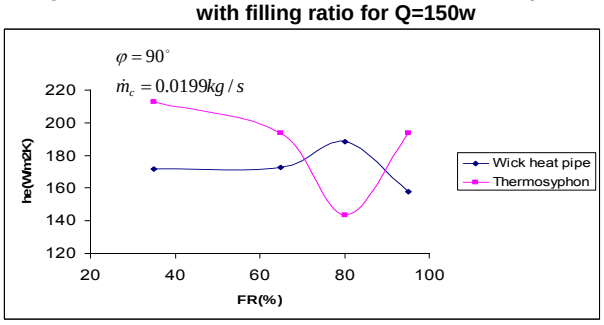

Fig. 8. Variation of heat transfer coefficient of evaporator with filling ratio for Q=200w

Some cases like solar applications, aerospace devices or microelectronic cooling applications are mostly capillary driven and inclination angle is too important in buoyancy forces in their performance. Furthermore in the absence of bulk forces (gravity, centrifugal, etc) in the axial direction, capillary forces pump the liquid axially through the wick, feeding liquid back to the evaporator in heat pipe. In order to optimize a collector orientation for any solar process for example, we need to know the effect of inclination angle in performance of the heat pipe and thermosyphon. This need motivated our present work.

Figs. 9,10 show that the inclination angle has a noticeable effect on the heat transfer coefficient of evaporator in the wick heat pipe and the thermosyphon.

Experiments are conducted by varying the inclination angle from the horizontal axis 30,50,70 and 90°. The maximum heat transfer coefficient was found in approximately 40° to 60° inclination angle from the horizontal direction in the thermosyphon.

The sudden decrease in heat transfer coefficient in the wick heat pipe and the gradual increase of heat transfer coefficient with increasing the inclination angle infer that the maximum heat transfer coefficient happened in more than 80°, albeit less accurate answer was found because of the fluctuation but the maximum heat transfer coefficient in the wick heat pipe occurred in higher inclination angle because of the fact that wick heat pipe had higher saturated vapor pressure in comparison with thermosyphon.

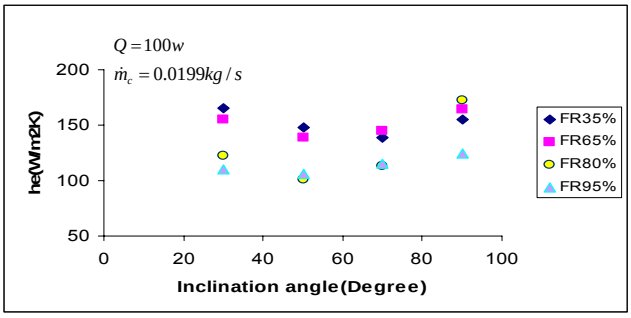

Fig. 9. Effect of inclination angle on evaporating heat transfer coefficient for wick heat pipe

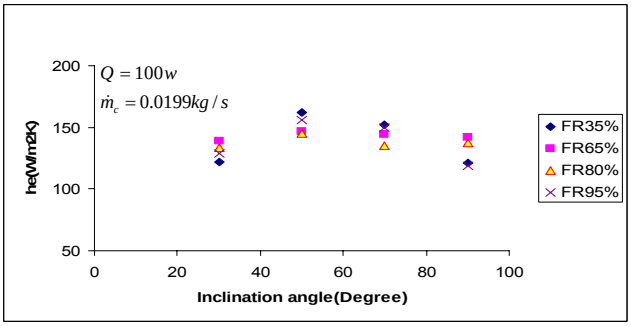

Fig. 10. Effect of inclination angle on evaporating heat transfer coefficient for thermosyphon

Fig.11 shows the comparison between heat transfer coefficient using Eqs. (6),(8) for FR35%, $\phi = 90^\circ$ and the experimental results where a good agreement is observed in the thermosyphon. The minimum value of differences in heat transfer coefficients was obtained at heat input 100w.

Research work on normal operating conditions of an inclined heat pipe with methanol as working fluid and screen mesh as capillary wick structure is quite scarce.

Fig.11 includes not only comparison between results of our experiment for the thermosyphon but also is a undeniable validation for wick heat pipe results. Therefore it remains virtually essential to compare results of the wick heat pipe with the thermosyphon.

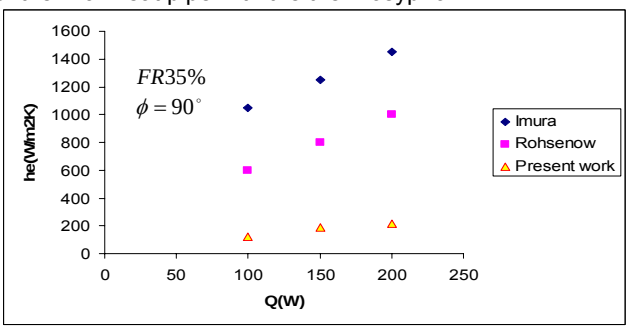

Fig. 11.Comparison between results of experiment and Eqs.(6),(8)

2.5.4. Heat transfer coefficient of condenser

Figs. 12 and 13 present the variation of heat transfer coefficient of the condenser with respect to the different inclination angle. As shown in the figures the maximum heat transfer of the condenser for the thermosyphon take place at $40^\circ \le \phi \le 60^\circ$ and for wick heat pipe occur at $60^\circ \le \phi \le 80^\circ$. As mentioned earlier, due to the existence of the wick the mean temperature difference between condenser and adiabatic section is lower than the thermosyphon. Consequently the heat transfer coefficient of the wick heat pipe increased.

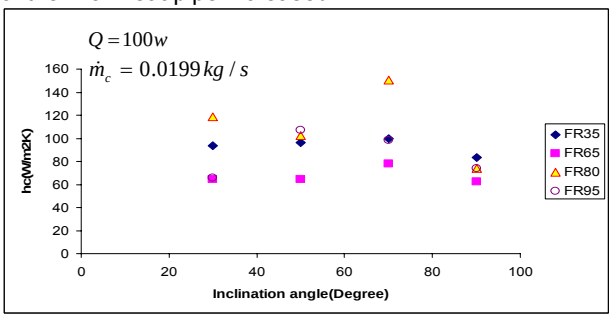

Fig. 12. Effect of inclination angle on condensing heat transfer coefficient for wick heat pipe

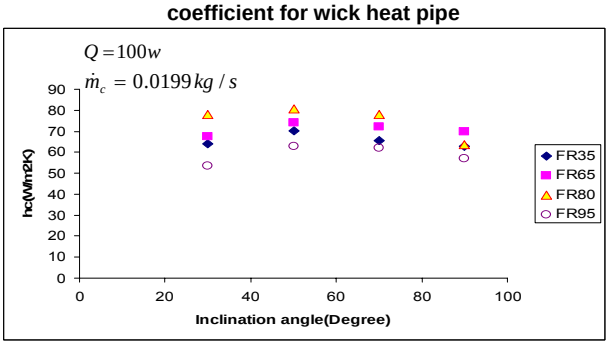

Fig. 13. Effect of inclination angle on condensing heat transfer coefficient for thermosyphon

The heat transfer coefficient of the condenser are presented in Figs.14,15 and 16 against the filling ratio for the different heat inputs. The behavior of condenser in the wick heat pipe is very similar to the ones observed in evaporator. This means that extended surface of the wick in the condenser made more vapor condensate. Relative to this simple reason, the greater working fluid inventory was, the higher condensation was. Moreover, as filling ratio and heat input increased, the heat transfer coefficient of the condenser was considerably increased.

As shown in the indicated Figs., it is definite that the heat transfer coefficient of condenser is maximum when $65\% \le FR \le 80\%$ for the thermosyphon and this value is $FR \ge 80\%$ for the wick heat pipe.

As a clear consequence, further increase in heat input led to increasing vapor pressure in a higher filling ratio in the condenser section and it decreased temperature difference between the adiabatic and the condenser section. Therefore the maximum heat transfer coefficient of condenser shifted to higher filling ratio. Moreover As the heat flux increases, the operating (vapor) temperature of the heat pipe increases, increasing the vapor pressure which compresses the non-condensable gases and thereby increasing the active region of the condenser.

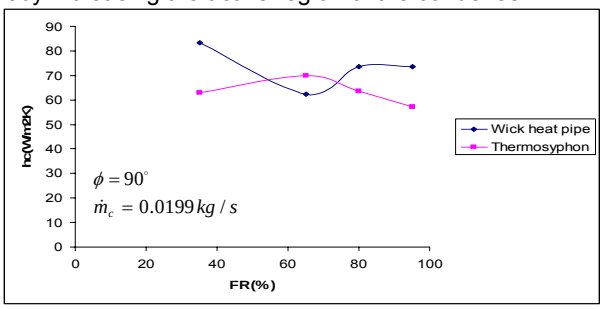

Fig. 14. Variation of heat transfer coefficient of condenser with filling ratio for Q=100w

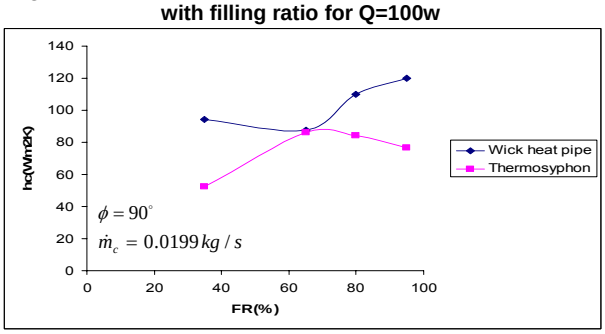

Fig. 15. Variation of heat transfer coefficient of condenser with filling ratio for Q=150w

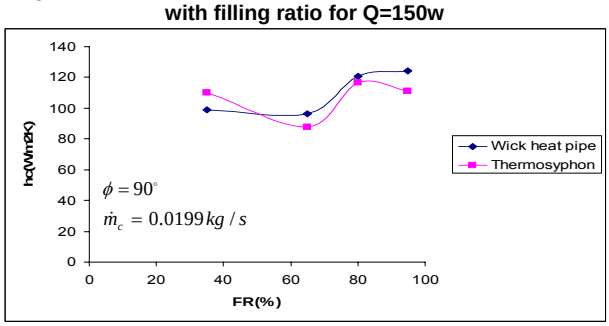

Fig. 16. Variation of heat transfer coefficient of condenser with filling ratio for Q=200w

2.5.5. Efficiency

The efficiency of wick heat pipe and thermosyphon is defined as the ratio of the output heat transfer from the condenser to the input heat transfer to the evaporator. Figs.17,18,19 and 20 show the efficiency variation with filling ratio in different inclination angles. As seen from these figures, the wick heat pipe generally had better efficiency than the thermosyphon. However it should be noted that the thermosyphon had higher efficiency since it was used in vertical position in $55\% \le FR \le 70\%$ .Additionally in this filling ratio the efficiency decrease dramatically in the wick heat pipe. The low value of efficiency for the wick heat pipe in comparison with the thermosyphon in $\phi = 90^\circ$ was attributed to wick resistance. This crucial factor was large enough to overcome the other growing efficiency parameters.

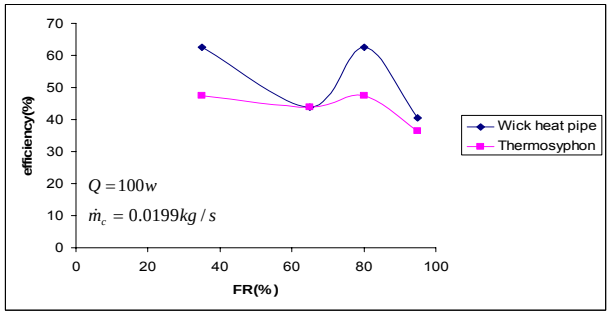

Fig. 17. Variation of efficiency with filling ratio for $\phi = 30^\circ$

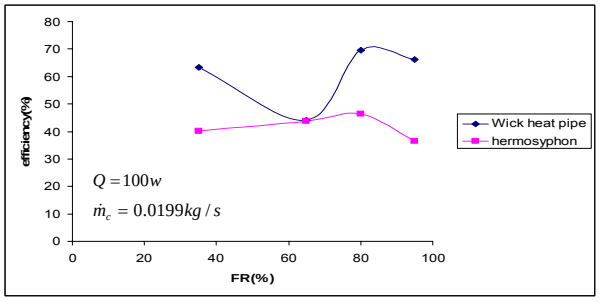

Fig. 18. Variation of efficiency with filling ratio for $\phi = 50^\circ$

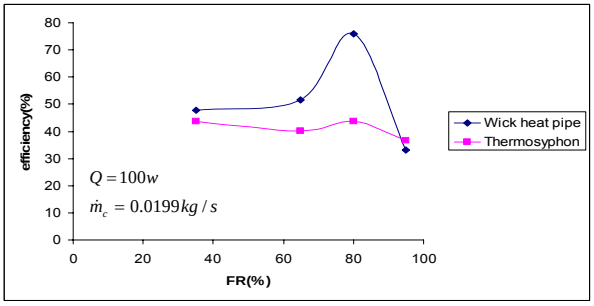

Fig. 19. Variation of efficiency with filling ratio for $\phi = 70^\circ$

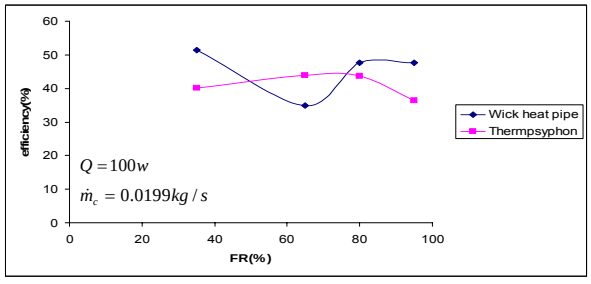

Fig. 20. Variation of efficiency with filling ratio for $\phi = 90^\circ$

2.6. A new correlation for heat transfer coefficient of evaporator and condenser in heat pipe

The parameters such as filling ratio (FR), inclination angle (φ), heat input (Q) and coolant mass flow rate $(\dot{m}_c)$ can effect the heat transfer coefficient of evaporator and condenser sections. By doing many experiments and changing these parameters, heat transfer coefficient of evaporator and condenser were calculated and a new equation for these coefficients were proposed. The new equation for h_e and h_c is as :

$$h_e = a(Q) + b(\dot{m}_c) + c(FR) + d(\phi) + e \qquad (21)$$

$$h_c = f(Q) + g(\dot{m}_c) + h(FR) + i(\phi) + j \qquad (22)$$

a,b,c,d,e,f,g,h,i,j obtained from the DataFit program.

In these equations, considering all parameters and using DataFit software" version 9.05.59", (DataFit is a science and engineering tool that simplifies the tasks of data plotting, regression analysis "curve fitting" and statistical analysis). DataFit proposed best fit model as:

$$h_e = 0.3148\ (Q) - 754\ .708\ (\dot{m}_c) - 30\ .57\ (FR) + 0.28\ (\phi) + 124\ .01 \quad (23)$$

$$h_c = 0.241\ (Q) - 2604\ .3(\dot{m}_c) + 10\ .143\ (FR) - 0.0989\ (\phi) + 117\ .237 \quad (24)$$

Fig.21 shows good agreement between results for heat transfer coefficient of evaporator and Fig.22 shows the agreement for heat transfer coefficient of condenser section.

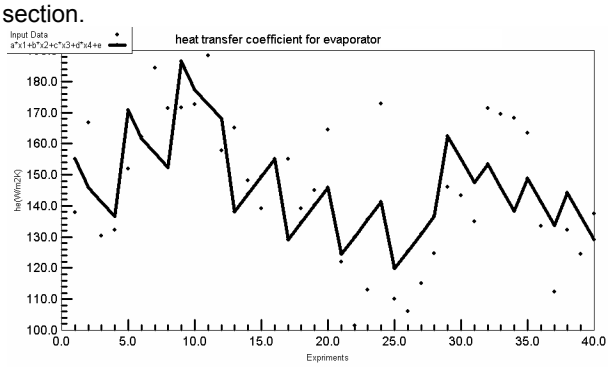

Fig. 21. Agreement between results of experiments and Eq.(23)

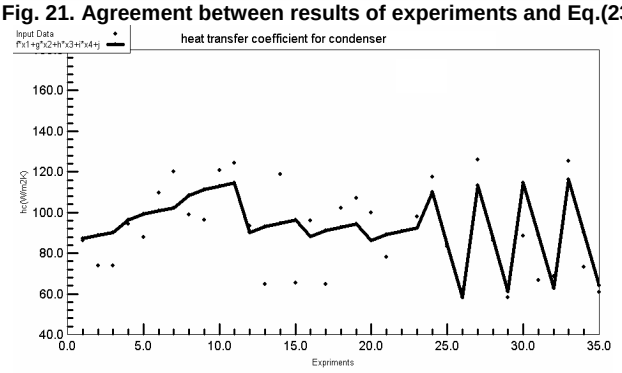

Fig. 22. Agreement between results of experiments and Eq.(24)

3. Conclusions

In this study, the effects of filling ratio $(35\% \le FR \le 95\%)$, Inclination angle $(30^\circ \le \varphi \le 90^\circ)$, heat input $(100w \le Q \le 200w)$ and coolant flow mass rate $(0.0099\ {kg}/{s} \le \dot{m}_c \le 0.0299\ {kg}/{s})$ on heat transfer characteristics of the 16mm inside diameter heat pipe with and without wick has been investigated. It has been found that :

1. This heat pipe with the methanol as working fluid and three layer wick structure is in normal operation in order to calculate different limitation such as capillary limit based on the steady state temperature.

2. The temperature distribution along the heat pipe is smooth in comparison with the heat pipe without wick or thermosyphon.

3. The heat transfer coefficient of evaporator increased as heat input increased.

4. The maximum heat transfer coefficient of evaporator happened in $80^\circ \le \varphi$ for the wick heat pipe and in $40^\circ \le \varphi \le 60^\circ$ for the thermosyphon.

5. The maximum heat transfer coefficient of condenser happened in $60^\circ \le \varphi \le 80^\circ$ for the wick heat pipe and in $40^\circ \le \varphi \le 60^\circ$ for the thermosyphon.

6. The maximum heat transfer coefficient of condenser happened in $80\% \le FR$ for the wick heat pipe and in $65\% \le FR \le 80\%$ for the thermosyphon.

7. The wick heat pipe generally had better efficiency than the thermosyphon. However the thermosyphon had higher efficiency since it was used in vertical position in $55\% \le FR \le 70\%$.

8. A new correlation for heat transfer coefficient of evaporator and condenser have been proposed and there are good agreements with results of experiment and results of these correlations achieved.

References

[1] Faghri A.,Heat pipe science and technology, Tylor and Francis, USA, 1995.

[2] Dunn, P., and Reay, A., Heat pipe, third edition, Pergamon Press, Oxford, U.K., 1982.

[3] A.Bejan, Convection Heat Transfer, second edition,1995.

[4] S.W.Chi, Heat Pipe Theory and Practice, McGraw-Hill, New York, 1976.

[5] Rohsenow,W.M. (1962) A method of correlating heat transfer data for surface boiling of liquids, Trans. ASME , 84, pp.969-974.

[6] Imura, H. Sasaguchi ,K. and Kozai, H. (1983)Critical heat flux in a closed two phase thermosyphon, Int. J. Heat Mass Transfer, 26(8), pp. 1181-1188.

[7] Busse, C. A. (1973). Theory of the ultimate heat transfer limit of cylindrical heat pipes. Int. J. Heat Mass Transfer 16.169.

[8] E. K .Levy, Theoretical investigation of heat pipes operating at low vapour pressure, ASME Journal of Engineering Industry 90(1968)547-522.

[9] S. W. Chi, Heat Pipe Theory and Practice, Hemisphere Publishing Corporation, Washington, DC, 1976, Chapters 2 and 3.

[10] V.P. Carey, Liquid-Vapor Phase-change Phenomena, Hemisphere Publishing Corporation, Washington, DC,1992, Chapter 6.